



## Vibrational Spectroscopy

Elixir Vib. Spec. 36 (2011) 3373-3387

Elixir  
ISSN: 2229-712X

# Computational studies on the structure, NBO, HOMO-LUMO analysis of the conformational states of 2-chloro-5-nitrobenzaldehyde based on *ab initio* and density functional theory studies

G. Santhi<sup>a</sup>, V. Balachandran<sup>b</sup> and V. Karpagam<sup>c</sup>

<sup>a</sup>Department of Physics, Government Arts College, Karur 639 005, India

<sup>b</sup>Department of Physics, A Government Arts College, Musiri 621 201, India

<sup>c</sup>Department of Physics, Srinivasan Polytechnic College, Peranbalur 621 212, India.

### ARTICLE INFO

#### Article history:

Received: 18 April 2011;

Received in revised form:

5 July 2011;

Accepted: 15 July 2011;

#### Keywords

2-chloro-5-nitrobenzaldehyde,

*Ab initio*,

DFT calculations,

FTIR, FT-Raman, NBO,

HOMO-LUMO,

Conformations,

Potential energy distribution.

### ABSTRACT

The solid phase FTIR and FT-Raman spectra of 2-chloro-5-nitrobenzaldehyde (CNB) have been recorded in the regions 4000–400  $\text{cm}^{-1}$  and 3500–100  $\text{cm}^{-1}$ , respectively. The optimized geometry, frequency and intensity of the vibrational bands, NBO analysis, HOMO- LUMO study of CNB in two conformational states of  $C_1$  and  $C_2$  obtained by the *ab initio HF* and DFT levels of theory using B3LYP/6-31G\*\* basis set. The harmonic vibrational frequencies were calculated and the scaled values have been compared with experimental FTIR and FT-Raman spectra. A detailed interpretation of the vibrational spectra of the title compound has been made on the basis of the calculated potential energy distribution (PED). Stability of the molecule arising from hyperconjugative interactions leading to its bioactivity, charge delocalization have been analyzed using natural bond orbital (NBO) analysis. The calculated HOMO-LUMO energies shows that charge transfer occur with in the molecule. The observed and calculated frequencies are found to be in good agreement.

© 2011 Elixir All rights reserved.

### Introduction

Benzaldehyde and its derivatives are currently finding increasing applications for several reasons. We will concentrate on this work on benzaldehydes, containing benzene ring with an aldehyde substituent. It is the simplest representative of the aromatic aldehydes. Benzaldehyde derivatives are among the most interesting carbonyl containing system and they are used chiefly in the synthesis of other organic compounds, ranging from pharmaceuticals to plastic additives. Due to the highly interesting nature of the aldehydic group with the surrounding media and conjugation of the aldehydic group with the surrounding media and conjugation of the phenyl ring, they are important intermediates for the processing of perfume and flavouring compounds and in the preparation of certain aniline dyes [1-3]. They also exhibit an important role on the rate of hydrogen evolution in lead acid batteries, as the rate of hydrogen evolution depends on the polarity of the environment [4].

Recent spectroscopic studies of the benzaldehyde and their derivatives have been motivated because the vibrational spectra are very useful for the understanding of specific biological process and for the analysis of relatively complex systems. Many important compounds are aromatic in part, including the steroidal hormone estone and the analgesic ibuprofen [5]. Benzene itself causes a prolonged exposure and should not be used as a laboratory solvent.

Aldehyde synthesis consists in treating an aromatic compound with a mixture of hydrogen cyanide and hydrogen chloride. Benzene and its derivatives are used extensively in agricultural applications as a disinfectant. These compounds are used as cosmetic agents, cutting oils, soap or synthetic

detergents, stabilizers, film forming materials and the like, and are widely used for protecting against or controlling microorganisms from a wide variety of fungi, bacteria, algal, viruses and yeasts. The preferred uses of the compositions are to protect wood, paint, adhesive, glue, paper, textile, leather, cardboard, lubricants, cosmetics, food caulking, feed caulking, feed and industrial cooling water from microorganisms. Hydroxy benzaldehyde synthesis consists in treating a phenol with chloroform in the presence of alkali followed by hydrolysis.

Benzaldehyde is used in perfumes, soaps, foods, drinks and other products; as a solvent for oils, rains, some cellulose ethers. Cellulose acetate and cellulose nitrate in the production of derivatives that are employed in the perfume and flavor industries in photo chemistry; as a corrosion inhibitor and dyeing auxiliary in the electroplating industry; and in the production of agricultural chemicals [6-7]. Benzaldehyde exists in nature occurring in combined and uncombined forms in many plants.

The best known natural source of benzaldehyde is amygdalin. Benzaldehyde is also the main constituent of the essential oils obtained by processing the kernel's of peaches, cherries, apricots and other fruits [7].

The assignments of band in the vibrational spectra of molecule are an essential of band in the vibrational spectroscopy for solving various structural chemical problems.

In the present study, the detailed vibrational analysis of the title compound was performed by combining the experimental and theoretical information using *ab initio* and Pulay's density functional theory (DFT) [8].

### Experimental Details

The sample CNB in the solid form was provided by the Lancaster Chemical Company, (UK) with a purity of greater than 98% and it was used as such without further purification. The FT-IR spectrum of NBEP was recorded in the frequency region 400–4000 cm<sup>-1</sup> on a NEXUS 670 spectrophotometer equipped with an MCT detector, a KBr pellet technique. The FT-Raman spectrum of NBEP has been recorded in the frequency region 100–3500 cm<sup>-1</sup> on a NEXUS 670 spectrophotometer equipped with Raman module accessory with Nd:YAG laser operating at 1.5W power continuously with 1064 nm excitation.

### Computational Details

Density functional calculations were carried out for CNB with the 2009 version (G09 – HF/DFT) of the GAUSSIAN suite programs [9] at the Becke-3-Lee-Yang-Parr (B3LYP) functional [10,11] implemented with the standard 6-31G\*\* basis set. All the parameters were allowed to relax and all the calculations converged to an optimized geometry which corresponds to a true energy minimum, as revealed by the lack of imaginary values in the wave number calculations. The Cartesian representation at the theoretical force constants have been computed at the fully optimized geometry by assuming the molecule belongs to Cs point group symmetry. The transformations of force field from Cartesian to internal local symmetry coordinates, the scaling, the subsequent normal coordinate analysis (NCA), calculation of potential energy distribution (PED) were done on a PC with the version G77 of the MOLVIB program written by Sundius [12,13].

### Prediction of Raman intensities

The Raman activities (S<sub>i</sub>) calculated with the GAUSSIAN-09 Program and adjusted during the scaling procedure with MOLVIB were converted to relative Raman intensities (I<sub>i</sub>) using the following relationship derived from the basic theory of Raman scattering [14-16].

where  $\nu_0$  is the exciting frequency (in cm<sup>-1</sup> units),  $\nu_i$  is the vibrational wavenumber of the *i*th normal mode, *h*, *c* and *k<sub>B</sub>* are universal constants, *T* is the temperature and *f* is the suitably chosen common scaling factor for all the peak intensities. The simulated IR and Raman spectra have been plotted using pure Lorentzian band shapes with the full width half maximum (FWHM) of 10 cm<sup>-1</sup>.

Natural bond orbital analysis was also performed by the Gaussian suite of program at the B3LYP level of theory analysis transforms the canonical delocalized Hartree Fock (HF) MOs into localized orbital's that are closely tied to chemical bonding concepts. This process involves sequential transformation of non orthogonal atomic orbital's (AOs) to the sets of natural atomic orbital's (NAOs), natural hybrid orbital's (NHOs) and NBOs. Natural bond orbital analysis gives the accurate possible natural Lewis structure picture of orbital because all orbital are mathematically chosen to include the highest possible percentage of the electron density. Interaction between both filled and virtual orbital spaces information correctly explained by the NBO analysis, it could enhance the analysis of intra-and inter-molecular interactions. The interaction between filled and antibonding orbital's represent the deviation of the molecule from the Lewis structure and can be used as the measure of delocalization. This noncovalent bonding–antibonding interaction can be quantitatively described in terms of the second order perturbation interaction energy (E(2)) [17–20]. This energy represents the estimate of the off-diagonal NBO Fock

Matrix elements. It can be deduced from the second order perturbation approach [21];

where  $q_i$  is the *i*th donor orbital occupancy, the diagonal elements (orbital energies) and *F* (*j,i*) the off diagonal NBO Fock Matrix element.

### Hyperpolarizability

The first hyperpolarizability ( $\beta$ ) of this novel molecular system and related properties ( $\beta$ ,  $\alpha$  and  $\Delta\alpha$ ) of CNB were calculated using B3LYP/6-31G\*\* basis set, based on the finite-field approach. In the presence of an applied electric field, the energy of a system is a function of the electric field. Polarizabilities and hyperpolarizabilities characterize the response of a system in an applied electric field [22]. They determine not only the strength of molecular interactions (long-range inter induction, dispersion force, etc.) as well as the cross sections of different scattering and collision process but also the nonlinear optical properties (NLO) of the system [23, 24]. First hyperpolarizability is a third rank tensor that can be described by 3×3×3 matrix. The 27 components of the 3D matrix can be reduced to 10 components due to the Kleinman symmetry [25]. It can be given in the lower tetrahedral format. It is obvious that the lower part of the 3×3×3 matrixes is a tetrahedral. The components of  $\beta$  are defined as the coefficients in the Taylor series expansion of the energy in the external electric field. When the external electric field is weak and homogeneous, this expansion becomes:

$$E = E^0 - \frac{\mu_i F_i}{1!} - \frac{\alpha_{ij} F_i F_j}{2!} - \frac{\beta_{ijk} F_i F_j F_k}{3!} - \frac{\gamma_{ijkl} F_i F_j F_k F_l}{4!} + \dots$$

where  $E^0$  is the energy of the unperturbed molecules,  $F\alpha$  the field at the origin  $\mu\alpha$ ,  $\alpha\alpha\beta$  and  $\beta\alpha\beta\gamma$  are the components of dipole moment, polarizability and the first hyperpolarizabilities, respectively.

The total static dipole moment is

$$\mu = (\mu_x^2 + \mu_y^2 + \mu_z^2)^{\frac{1}{2}}$$

The isotropic polarizability is

$$\alpha = \frac{\alpha_{xx} + \alpha_{yy} + \alpha_{zz}}{3}$$

The polarizability anisotropy invariant is

$$\Delta\alpha = 2^{-\frac{1}{2}} [(\alpha_{xx} - \alpha_{yy})^2 + (\alpha_{yy} - \alpha_{zz})^2 + (\alpha_{zz} - \alpha_{xx})^2 + 6\alpha_{xz}^2]^{\frac{1}{2}}$$

$$\beta_{tot} = (\beta_x^2 + \beta_y^2 + \beta_z^2)^{\frac{1}{2}}$$

$$\beta_x = \beta_{xxx} + \beta_{yyx} + \beta_{zzx}$$

$$\beta_y = \beta_{yyy} + \beta_{xyy} + \beta_{zyy}$$

$$\beta_z = \beta_{zzz} + \beta_{xzz} + \beta_{yzz}$$

and the average hyperpolarizability is

$$\beta_{tot} = (\beta_x^2 + \beta_y^2 + \beta_z^2)^{\frac{1}{2}}$$

where *E* is the energy of the unperturbed molecules, *F<sub>i</sub>* is the field at the origin and  $\mu_i$ ,  $\alpha_{ij}$ ,  $\beta_{ijk}$  and  $\gamma_{ijkl}$  are the components of dipole moment, polarizability, first hyperpolarizabilities and the second hyperpolarizabilities, respectively. The total static dipole moment  $\mu$ , the mean polarizability  $\alpha_{av}$ , the anisotropy of the polarizability and the first hyperpolarizability  $\beta_{tot}$  using the *x*, *y* and *z* components, are defined. The B3LYP/6-31G\*\* calculated the first hyperpolarizability of CNB is 5.5010×10<sup>-31</sup>esu. The total molecular dipole moment ( $\mu$ ), mean polarizability ( $\alpha_{av}$ ) and anisotropy polarizability ( $\Delta\alpha$ ) of CNB molecule have been

collected in Table 1, but the experimental evaluation of this data is not readily available. When compared hyperpolarizability of other molecules reported earlier [42, 43], the value of first hyperpolarizability of CNB molecule possesses nonlinear optical properties that can be used for nonlinear optical applications.

## Results and Discussion

### Molecular geometry

The molecular structure with labeling of atoms of 2-chloro-5-nitrobenzaldehyde and the two anticipated conformers are shown in Fig. 1. From the spectral point of view of the molecule belongs to  $C_s$  point group symmetry the 42 fundamental modes of vibrations of CNB are distributed to  $29A'$  and  $13A''$  species. The  $A'$  and  $A''$  species represent the in-plane and out-of-plane vibrations, respectively. The bond lengths and bond angles calculated by means of B3LYP method for the title compound (both conformers) are depicted in Table 2. The DFT structure optimizations of CNB have shown that conformer C2 (s-trans) has a significantly lower energy ( $E = -1009.6583$  Hartress) than the conformer C1 (s-cis) ( $E = -1009.6466$  Hartress), the subsequent force field and vibrational frequency calculations performed at the B3LYP/6-31G\*\* level of theory [26] for both optimized structures of CNB.



**Fig. 1** The molecular structure with labeling of atoms of 2-chloro-5-nitrobenzaldehyde and the two anticipated conformers

Normal coordinate analysis is the mathematical procedure that gives the normal coordinates, their frequencies and force constants. The detailed description of vibrational modes can be given by means of normal coordinate analysis. The internal coordinates describe the position of the atoms in terms of distances, angles and dihedral angles with respect to an origin atom. The symmetry coordinates are constructed using the set of internal coordinates. In this study, the full set of 54 standard internal coordinates (containing 12 redundancies) for CNB was defined as given in Table 3. From these, a non-redundant set of local symmetry coordinates were constructed by suitable linear combinations of internal coordinates following the recommendations of Fogarasi et al. [27] are presented in Table 4.

The optimized geometries of the title molecule at HF and DFT level theories compared with the experimental geometries of the similar molecule [44, 45, 46] based on X-ray diffraction data are presented in Table 2. From the theoretical values, it is found that most of the optimized bond lengths are slightly larger than the experimental values. The phenyl ring appears little distorted and angles slightly out of perfect hexagonal structure. It is due to the substitutions of the chlorine atom, NO<sub>2</sub> group in the place of H atoms. The breakdown of hexagonal symmetry of the benzene ring is obvious from the elongation of C2–C3 (1.387Å) and C1–C2 (1.391Å) from the remaining C5–C6 (1.375Å) and C3–C4 (1.379Å) bond lengths since the replacement of chlorine atom, nitro group with different masses. The order of the optimized bond lengths of the six C–C bonds of the ring as C5–C6 < C4–C5 < C3–C4 < C2–C3 < C1–C6 < C1–C6. The C–Cl bond distance of cal. 1.739Å is just 0.005Å lower than the reported experimental value of 1.734Å for CNB. The order of the optimized bond angles as C6–C1–C7 < C2–C1–C6 < C2–C3–C4 < C1–C2–C3 < C2–C1–C7.

### Potential energy distribution

To check whether the chosen set of symmetric coordinates contribute maximum to the potential energy associated with the molecule, the PED has been carried out. The vibrational problem was set-up in terms of internal and symmetry coordinates. The geometrical parameters of the molecule were allowed to relax and all the calculations converged to an optimized geometry which corresponds to a true minimum, as revealed by the lack of imaginary values in the theoretical force constants have been computed at the fully optimized geometry by assuming  $C_s$  point group symmetry.

The symmetry of the molecule was also helpful in making vibrational assignment. The transformation force field, subsequent normal coordinate analysis and calculation of the PED were calculated by using MOLVIB program [12, 13] B3LYP/6-31G\*\* are also presented in Table 5.

### Computed IR intensity and Raman activity analysis

Computed vibrational spectral IR intensities and Raman activities of the title molecule for corresponding wave numbers by HF and DFT methods with B3LYP With 6-31G\*\* basis set have been collected in Table 5. The comparative graphs of IR intensities and Raman activities to observed frequency for the basis set 6-31G\*\* are shown in Fig. 2 and Fig. 3, respectively.

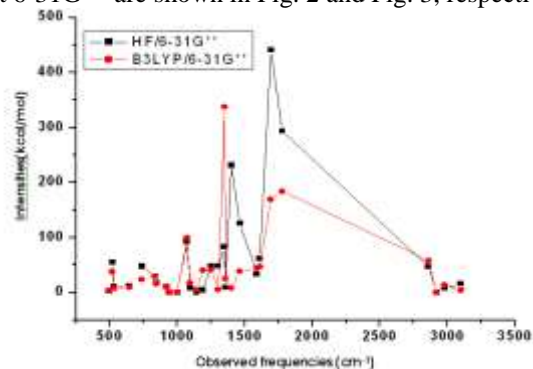


**Fig.2** The comparative graph of IR intensities to observed frequency

### Computed vibrational frequency analysis

The comparative graph of calculated vibrational frequencies by HF and DFT methods at 6-31G\*\* basis set for the title molecule is given in Fig. 4. From the figure, it was found that the calculated (scaled) frequencies by B3LYP with 6-

31G\*\* basis set is closer to the experimental frequencies than HF method with 6-31G\*\* basis set.

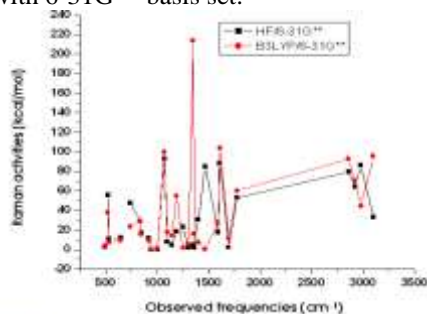


**Fig.3** The comparative graph of Raman activities to observed frequency

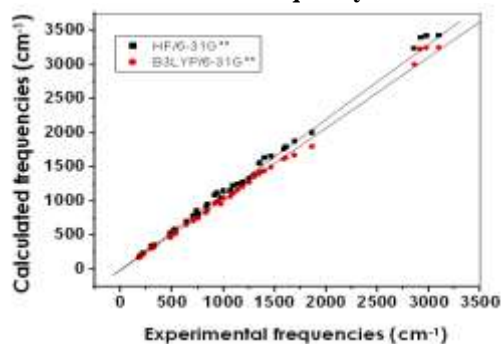


**Fig.4** The comparative graph of calculated vibrational frequencies by HF and DFT methods at 6-31G\*\* basis set

Comparing bond angles and bond lengths of B3LYP at 6-31G\*\* level with those of HF, as a whole the formers are bigger than later and the B3LYP calculated values correlates well compared with the experimental data. Although the differences, calculated geometrical parameters represent a good approximation and they are basis for the calculating other parameters, such as vibrational frequencies and thermodynamics properties.

#### Vibrational spectral analysis

A detailed analysis of the vibrational frequencies has been performed with the computed data obtained at HF and DFT B3LYP/6-31G\*\* and the results are presented in Table 5. The relative intensities of IR and Raman active vibrations are calculated from the Computed data and these listed in Table 5. The FTIR and FT-Raman spectra of CNB are shown in Figs. 5 and 6, respectively.

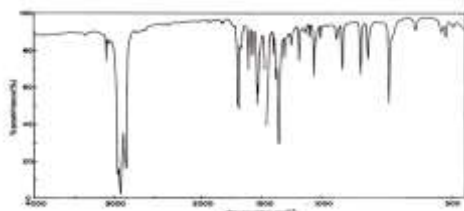


**Fig.5** Observed FT-IR spectrum of 2-chloro-5-nitrobenzaldehyde

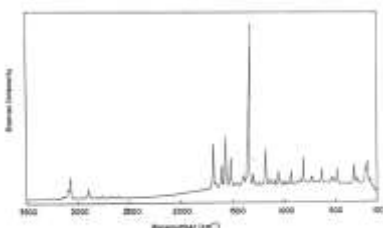


**Fig.6** Observed FT-Raman spectrum of 2-chloro-5-nitrobenzaldehyde

#### Aldehyde group vibrations

The CH stretching vibrations of the aldehyde group usually appear in the region 2820–2850 cm<sup>-1</sup>. The weak band observed in the FTIR spectrum at 2860 cm<sup>-1</sup> is due to CH stretching vibration of the aldehyde group. The in-plane CH deformation made of aldehyde group is observed at 1400 cm<sup>-1</sup> with weak intensity in the FTIR spectrum. The carbonyl (C=O) stretching vibrations in the substituted benzaldehyde is reported near 1795 cm<sup>-1</sup> [28]. The very strong band centered at 1610 and 1608 cm<sup>-1</sup> in both FTIR and laser Raman Spectra are attributed to C=O stretching vibrations of the aldehyde group [30]. Hence the weak band observed at 324 cm<sup>-1</sup> could be assigned to C=O in-plane bending vibration have assigned C=O band at 122 cm<sup>-1</sup> in the Raman spectrum of chlorobenzaldehyde as aldehyde out-of-plane wagging. In CNB, the weak band centered at 188 cm<sup>-1</sup> in the Raman spectrum could be due to aldehyde out-of-plane wagging vibration. A weak to medium intensity band due to the aldehydic group –CHO deformation vibration is found in the region 1034–966 cm<sup>-1</sup>. In consonance with this, the weak intensity band at 920 cm<sup>-1</sup> could be assigned to CHO out-of-plane deformation. The bands at 740 and 743 cm<sup>-1</sup> are attributed to CC (CHO) out-of-plane vibrations.

Intra- and inter molecular factors affect the carbonyl absorption [29, 30] in common organic compounds. Inductive and mesomeric effects associated with the groups attached to the carbonyl group shift significantly the carbonyl absorption in carbonyl compounds such as aldehydes. The wave number of absorption due to the carbonyl group depends mainly on the force constant, which in turn depends upon inductive effect, conjugative effect, field effect and steric effect. The inductive effect reduces the length of the C=O bond and thus increase its force constant and consequently the wave number of absorption [30].

#### C–H Vibrations

For simplicity, modes of vibrations of aromatic compounds are considered as separate C–H or ring C–C vibrations. However, as with any complex molecules, vibrational interactions occur and these levels only indicate the predominant vibration. Substituted benzenes have large number of sensitive bands, that is, bands whose position is significantly affected by the mass and electronic properties, mesomeric or inductive of the substituents. Accordingly to the literature [31, 32], in infrared spectra most mono nuclear and poly nuclear aromatic compounds have three or four peaks in the region 3000–3100 cm<sup>-1</sup>, these are due to the stretching vibrations of the ring CH bands. Accordingly, in the present study, the FT-IR bands identified at 3100, 2980, 2920 cm<sup>-1</sup> and FT Raman band at 3096, 2917 cm<sup>-1</sup>, are assigned to C–H stretching vibrations of CNB. The FT-IR bands at 1465, 1400, 1252 cm<sup>-1</sup> and the FT Raman band at 1397 cm<sup>-1</sup> were assigned to C–H in-plane bending vibration of CNB. The C–H out-of-plane bending vibration of the title compound were well indentified at 1002, 942, 920 cm<sup>-1</sup> in the FT-IR and 1004, 945 cm<sup>-1</sup> in the FT-Raman spectra are found to be well within their characteristic region.

#### C – C vibrations

The ring C=C and C–C stretching vibrations, known as semicircle stretching usually occurs in the region 1400-1625 cm<sup>-1</sup> [33-35]. Hence in the present investigation, the FT-IR bands indentified at 1610, 1590, 1351, 1303, 1190, 1098 cm<sup>-1</sup> and FT-Raman bands at 1608, 1586, 1357, 1304, 1193, 1100, 1072 cm<sup>-1</sup> are assigned to C–C stretching vibrations of CNB. The C–C

out-of-plane bending vibration of the title compound identified at 498 cm<sup>-1</sup>. These observed frequencies show that, the substitutions in the ring to some extent effect the ring modes at vibrations.

#### C-Cl vibrations

The vibrations belonging to the bond between the ring and the halogen atom are worth to discuss here, since mixing of vibrations are possible due to the lowering of molecular symmetry and the presence of heavy atoms on the periphery of the molecule [36]. In the present investigation (C-Cl) stretching vibrations observed at 521 cm<sup>-1</sup> Mooney [37, 38] assigned vibrations of C-X group (X=Cl,Br,I) in the frequency range 1129–280 cm<sup>-1</sup>. The ring halogen stretching mode were observed as strong Raman and weak to medium IR bands at 650–675 cm<sup>-1</sup> range for chlorine. As expected in our studies, the bands at 520 and 521 cm<sup>-1</sup> are assigned to C-Cl stretching vibration coupled with ring deformation vibration 521 cm<sup>-1</sup> coincides with experimental observation.

#### C-N Vibrations

The identification of C-N vibrations in the hetero cyclic ring is found to be a difficult task because if the mixing of several vibrations Using GAUSSVIEW visualization program we find that the C-N ring stretching corresponds to the frequency of 1320 cm<sup>-1</sup> whereas Yadav et al [39] assigned a value of 957 cm<sup>-1</sup> for the above C-N stretching during their experimental studies. Our calculation followed by GAUSSVIEW visualization showed the 821 cm<sup>-1</sup> frequency corresponding to a mixed stretching frequencies due to C-NO<sub>2</sub>. Other C-N out-of-plane bending vibrations are found to be at 568 cm<sup>-1</sup>

#### Nitro group vibrations

The nitro group has two identified NO bands that vibrate asymmetrically causing strong absorption in the region 1625–1510 cm<sup>-1</sup> and symmetrically resulting causing strong absorption in the region 1400–1360 cm<sup>-1</sup>. For the title compound (CNB) the asymmetric stretching vibrations of the NO<sub>2</sub> group are observed at 1695 and 1354 cm<sup>-1</sup> in the FTIR and FT-Raman, respectively. The band at 953 cm<sup>-1</sup> is assigned to the scissoring mode of the NO<sub>2</sub> group [40]. Aromatic nitro compounds have a band of weak to medium intensity in the [41] 590–550 cm<sup>-1</sup> due to in-plane deformation mode of rocking mode has been assigned at 295 cm<sup>-1</sup> in the FT Raman spectrum of the title compound. The NO<sub>2</sub> wagging mode observed at 740 cm<sup>-1</sup>, 730 cm<sup>-1</sup> in the FT Raman, FT-IR spectra respectively.

#### NBO analysis

The Table 6 shows that the first two columns give the type of orbital and occupancy between 0 and 2.000 electrons. The type can be bonding, lone pair and anti bonding. A normal Lewis structure would not have any anti-bonding orbital, so the presence of anti bonding orbital's shows deviation from normal Lewis structure. Anti-bonding localized orbital's are called non-Lewis NBO's. If the occupancy is not 2.000, then there is deviation from an ideal Lewis structure. The CNB molecule shows some deviations, otherwise it is well approximated using Lewis structure.

In this Table, BD (N13–O14) orbital with 1.99585 electrons has 48.19% N13 character in a sp<sup>2.10</sup> hybrid and has 51.81% O14 character in a sp<sup>2.67</sup> hybrid. The sp<sup>2.10</sup> hybrid on N has 67.69% p-character. The sp<sup>2.66</sup> hybrid on O has 72.40% p-character. An idealized sp<sup>2</sup> hybrid has 75% p-character. The BD (N13–O14) bond then corresponds roughly to the quantitative concept of interacting sp<sup>3</sup> hybrids. The two coefficients, 0.6942

and 0.7198 are called polarization coefficients. The sizes of these coefficients show the importance of the two hybrids in the formation of the bond. The oxygen has larger percentage of this NBO, at 51.81% and gives the larger polarization coefficient of 0.7198 because it has the higher electronegativity. Similarly BD (C2–Cl10), BD (C4–C5), BD (C5–N13), BD (C7–O8), BD (N13–O15), BD (N5–C6), BD (C6–N11), BD (C1–C2), bonding orbitals are also shows nitrogen and chlorine have the lesser percentage of NBOs and gives the lesser polarization coefficients as compare to BD (N13–O14) bond. This shows that nitrogen and chlorine in above bonding orbital have less electronegative as compare to BD (N13–O14). At the end of the table nitrogen and chlorine lone pair NBO's are expected to be Lewis structure.

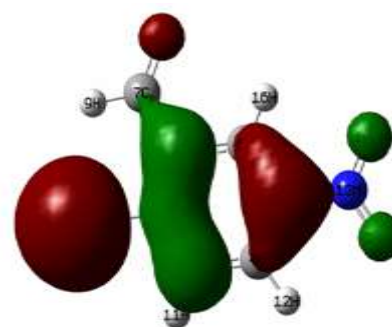
#### Perturbation theory energy analysis

Delocalization of the electron density between occupied Lewis type (bond (or) lone pair) NBO orbital's and formally unoccupied (antibond (or) Rydberg) non Lewis NBO orbital's corresponding to a stabilizing donor- acceptor interaction. The energy of this interaction can be estimated by the second order perturbation theory [21]. Table 7 lists the calculated second order interaction energies (E(2)) between the donor –acceptor orbital's in CNB.

The most important interaction energies, related to the resonance in the benzene ring are electron donating from the BD (C4–C5), BD (C6–H16), LPO14, LPO15, to the antibonding acceptor BD\* (N13–O14), BD\* (C4–C5), BD\* (C5–N13), BD\* (N13–O14), orbital's and their corresponding energies are 2.11, 4.32, 4.45, 4.46 kcal/mol, respectively. These interactions clearly indicate the strongest stabilization energy increase of electron delocalization occurs due to substitution of the molecule.

#### HOMO - LUMO band gap

The conjugated molecules are characterized by a highest occupied molecular orbital-lowest unoccupied molecular orbital (HOMO-LUMO) separation, which is the result of a significant degree of ICT from the end-capping electron-donor groups through  $\pi$ -conjugated path. The strong charge transfer interaction through  $\pi$ -conjugated bridge results in substantial ground state donar-acceptor mixing and the appearance of a charge transfer band in the electronic absorption spectrum of a charge transfer band in the electronic absorption spectrum. Therefore, an ED transfer occurs from the more aromatic part of the  $\pi$ -conjugated system in the electron-donor side to its electron-withdrawing part the atomic orbital components of the frontier molecular orbitals are shown in Fig 7. The HOMO-LUMO energy gap value is found to be  $\square$ 0.17595 a.u. which is responsible for the bioactive property of the compound chloro nitrobenzaldehyde.



(a) EHOMO= $\square$ 0.27894 a.u

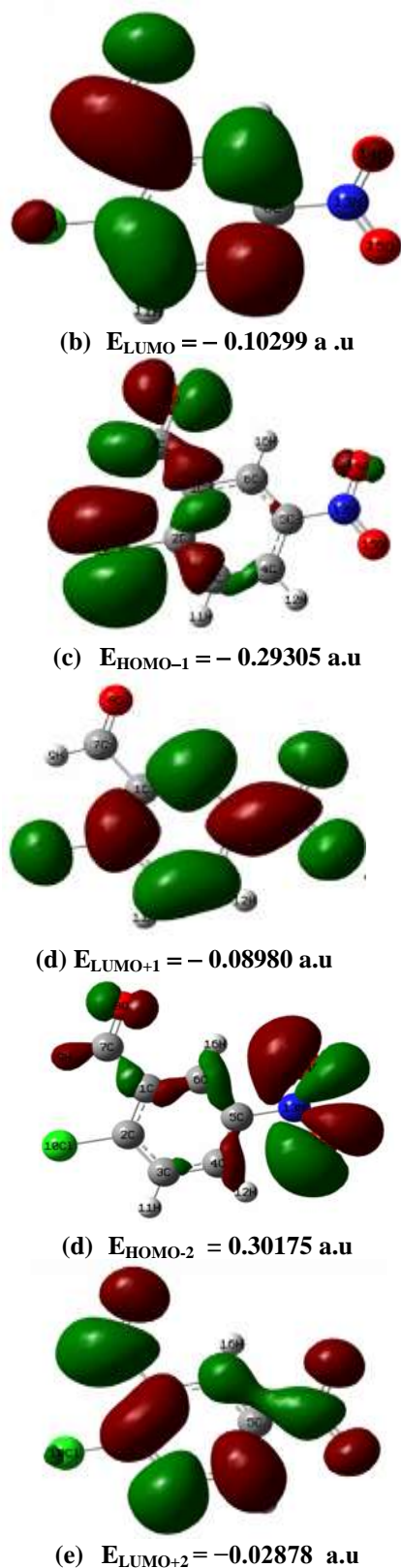


**Fig.7 Selected molecular orbital contours of 2-chloro-5-nitrobenzaldehyde**

The Fig. 7 shows molecular orbitals from HOMO-2 to LUMO+2 of the title molecule. In which all the LUMO surfaces are well localized within the phenyl ring. In other words all the ring component intramolecular interactions are mostly occurred in LUMO levels. LUMO+1 and LUMO+2 surfaces shown in (Figs. 7d, 7f) have no amplitude [42] on aldehyde group linked to six member ring of CNB. In HOMO-2, the orbitals have well localized on aldehyde group of CNB. In HOMO-2, H9 in

aldehyde group is highly coupled with C7 and C1. Moreover,  $H_9^+$  and  $O_8^-$  interaction is also present in this orbital. The most of surfaces shown in the HOMO side have no amplitude on phenyl ring but, all the HOMO surfaces (*see* Figs. 7a, 7c, 7e) have very high amplitude on aldehyde group of CNB.

The presence of intramolecular charge transfer from donor to acceptor group within molecule can identify by analyzing the co-existence of IR and Raman activity [43] itself. It is also observed that in our title molecule the bands at 3100, 1695, 1610, 1357, 1303, 1098, 740 and 521  $\text{cm}^{-1}$  in FT-IR spectrum have their counterparts in FT-Raman at 3096, 1695, 1608, 1357, 1304, 1100, 743 and 520  $\text{cm}^{-1}$  show that the relative intensities in IR and Raman are comparable resulting from the electron cloud movement through single-double bond  $\pi$  conjugated path from donor to acceptor groups. The analysis of wave function indicates that the electron absorption corresponds to the transition from the ground state to the first excited state and is mainly described by one-electron excitation from the Highest Occupied Molecular Orbital (HOMO) to the Lowest Unoccupied Molecular Orbital (LUMO). The HOMO, LUMO energies of CNB have been calculated at B3LYP/6-31G(d,p) level is presented in Table 8. The energy gap presented in Table 9 reflects the chemical activity of the molecule. HOMO represents the ability to donate an electron and LUMO represents the ability to accept an electron. Among the six subsequent excited states calculated, the strongest transitions appear between HOMO  $\rightarrow$  LUMO orbitals. The numerical value of energy gap between HOMO-LUMO orbitals calculated at B3LYP level is  $-0.17595 \text{ a.u.}$  The energy gaps for other possible energy transitions are presented in Table 9.

#### Conclusion

Quantum chemical calculations and vibrational spectral studies have been performed on CNB in order to identify its structural and bonding features responsible for its bioactivity. The normal mode frequencies and corresponding vibrational assignment of the title compound are examined theoretically using the Gaussian 09 package.

The optimized geometries and complete vibrational analysis of 2-chloro-5-nitrobenzaldehyde in two conformational states  $C_1$ ,  $C_2$  were performed and analyzed both at HF and DFT level of theories utilizing 6-311G (d, p) basis set.

The data obtained during the course of present investigation show that a better agreement between the experimental and computed data is obtained by using DFT method with a 6-31G\*\* basis set.

The high degree of stabilization emanating from strong mesomeric effects has been well demonstrated by NBO analysis. The second order perturbation theory results show that the  $\text{NO}_2$  group behave as separate unit with sufficient interaction energy. The lowering of HOMO-LUMO band gap supports bioactive property of the molecule.

#### References:

- [1] R. Narukula, D.E.G. Shukur, Y.Z. Xu, Nucleic Acids 33 Res(2005) 1767-1778.
- [2] D. Barcevic, S.Sosa, R.D.Loggia, A. Tubaro, B. Simonovska, A. Krana, A. Zupanicic, Journal of Ethnopharm 75 (2001) 125.
- [3] C.A. Liberko, J. Shearer, Journal of Chemical Education 77 (2000) 1204-1205.
- [4] Yu. Kamenev, A.V. Kiselevich, E.I. Ostapenko, V.N. Varypaev, Russian Journal of Applied Chemistry 77 (2004) 1455-1459.

- [5] N. Georgieva, V. Gadjeva, Tolakova Dimitrov D. *Pharmazie* 60 (2005) 138.
- [6] R. J. Lewis Sr. *Hawley's Condensed Chemical Dictionary*, (14<sup>th</sup> edn) John Wiley & Sons, (2002).
- [7] F. Bruhne et al., Benzaldehyde. In *Ullmann's Encyclopedia of Industrial Chemistry*(7<sup>th</sup> edn). JohnWiley & sons; (2005).
- [8] R. G. Parr, W Yang, *Density Functional Theory of Atoms and Molecules*, (Oxford, New York), (1989).
- [9] GAUSSIAN 09, Revision, A.02 GAUSSIAN, Inc, Pittsburg P.A, (2009).
- [10] A.D. Becke, *Journal of Chemical Physics Society* 98 (1993) 5648.
- [11] C. Lee, W. Yang, RC parr, *Physics Review B*37 (1988) 785–789.
- [12] T. Sundius, *Journal of Molecular Structure* 218 (1990) 321–326.
- [13] (a) T. Sundius, *Vibrational Spectroscopy* 29 (2002) 89–95; (b) MOLVIB, V.7.0: Calculation of Harmonic Force Fields and vibrational Modes of Molecules, QCPE Program No.807 (2002)
- [14] P.L. Polavarapu, *Journal of Physical Chemistry* 94 (1990) 8106–8112.
- [15] G. Keresztury, S. Holly.J. Varga,Besenyei, A.Y. Wang, J.R.Durig, *Spectrochimica Acta Part A* 49 (1993) 2007.
- [16] G. Keresztury, *Raman Spectroscopy: Theory*, in *Handbook of Vibrational Spectroscopy*, Vol.1, (Eds:Journal of Molecular Chalmers, P.R. Griffiths), John wiley and sons: 2002,P71.
- [17] A. E. Reed, F. Weinhold, *Journal Chemical Physics society* 83 (1985) 1736.
- [18] A. E. Reed, R.B. Weinstock, F. Weinhold, *Journal of Chemical Physics Society* 83 (1985)735.
- [19] A. E. Reed, F. Weinhold, *Journal Chemical Physics* 78 (1983) 4066.
- [20] J. P. Foster, F. Weinhold, *Journal of American Chemical Society* 102 (1980) 7211.
- [21] J. Chocholousova, V. Vladimir Spirko, P Hobza, *Chemical Physics society*, 2004, 6:37
- [22] V. Krishnakumar, G. Keresztury, T. Sundius, R. Ramasamy, *Journal of Molecular Structure* 702 (2004) 9–21.
- [23] P.L. Polavarapu, *Journal of Physical Chemistry*, 94 (1990) 8106–8112.
- [24] V. Krishnakumar, R. Mathammal, S. Muthunatesan, *Spectrochimca Acta Part A* 70 (2008) 201–209.
- [25] N.B. Colthup, L.H. Daly, S.E. Wiberley, *Introduction to Infrared and Raman Spectroscopy*, 13, 3rd edition, academic press, Boston, 1990.
- [26] P. Pulay, G. Fogarasi, G. Pongor, J.E. Boggs & A. Vargha, *Journal of Applied Chemical Society* 105 (1983) 7037–7047.
- [27] G. Fogarasi, X. Zhou, P.W. Taylor, P. Pulay, *Journal of American Chemical Society* 115 (1992) 819
- [28] P.K. Syed Tariq, Verma, Rashid Aquell, *Indian Journal of Pure and Applied Physics* 20 (1982) 974.
- [29] J. Mohan, *Organic Spectroscopy – Principles and Applications* (2<sup>nd</sup> edn) Narosa Publishing House, New Delhi,pp(30) (2011).
- [30] V. Krishnakumar, V. Balachandran, *Spectrochimica Acta Part 63* (2006) 464–476.
- [31] G. Socrates, *Infrared and Raman Characteristic Group frequencies*, 3<sup>rd</sup> edn., Wiley, New York(2001).
- [32] G. Eazhilarasi, R. Nagalakshmi, V. Krishnakumar, *spectrochimica Acta part A* 71 (2008) 502–507.
- [33] V. Krishnakumar, R. John Xavier, *Indian Journal of Pure and Applied physics* 41 (2003) 95–98.
- [34] K. Furic, V. Mohacek, M. Bonifacic, I. Stefanic, *Journal of Molecular Structure* (1992) 267–270.
- [35] N.P. Sing, R.A. Yadav, *Indian Journal of Physics B* 75(4) (2001) 347.
- [36] M. Bakilar, IV Maslov, S. Akyuz, *Journal of Molecular Structure*, 475 (1999) 83–92.
- [37] E. F. Mooney, *Spectrochimica Acta Part A* 20 (1964) 1021.
- [38] E. F. Mooney, *Spectrochimica Acta Part A* (1963) 877.
- [39] B. S. Yadav, Ali Israt, P Kumar, P. Yadav, *Indian Journal of Pure and Applied Physics* 45 (2007) 979–983.
- [40] Hari Ji Sing, Prinyanka Srinivastava, *Indian Journal of Pure and Applied Phisics* 47 (2009) 557–562.
- [41] H.G. Silver, J.L. Wood, *Trans Farady soc.* 60(1964).
- [42] Mama Nsangou, Nejme-Eddine Jaidane, Zohra Ben Lakhdar, *Internet Electronic of Journal of Molecular Design*, 5 (2006) 89–101.
- [43] P.L. Anto, Ruby John Anto, Hema Tresa Varghese, C. Yohannan Panicker, Daizy Philipe, *Journal of Raman Spectroscopy* 41 (2010) 113–119.
- [44] H. Mollendal, S. Gundersan, M.A. Tafipolsky, H.V. Volden, *Journal of Molecular Structure* 444 (1998) 47–56.
- [45] S. Samdal, T.G. Strand, M.A. Tafipolsky, L.V. VilKov, M.V Popik, H.V. Volden, *Journal of Molecular Structure*.435 (1997)89–99.
- [46] L.F. Shishkov, L.V. VilKov, I.Hargittai, *Journal of Molecular Structure*. 352/353 (1995)157–160.

**Table 1 The electric dipole moment  $\mu$  (Debye), the mean polarizability  $\alpha_{\square}$  ( $\times 10^{-22}$  esu), anisotropy polarizability  $\Delta\alpha$  ( $\times 10^{-25}$  esu) and first hyperpolarizability  $\beta_{\text{tot}}$  ( $\times 10^{-31}$  esu) for 2-chloro-5-nitrobenzaldehyde.**

Parameters	Values	Parameters	Values
$\mu_x$	-2.9312	$\beta_{xxx}$	-59.6228
$\mu_y$	-3.1785	$\beta_{yyy}$	-41.6295
$\mu_z$	0.00000	$\beta_{zzz}$	-0.0001
$\mu$	8.486	$\beta_{xyy}$	8.2907
$\alpha_{xx}$	-85.7551	$\beta_{xxy}$	3.6607
$\alpha_{xy}$	0.2905	$\beta_{xxz}$	0.0001
$\alpha_{xz}$	-0.0001	$\beta_{xzz}$	7.1315
$\alpha_{yy}$	-77.9206	$\beta_{yzz}$	5.2207
$\alpha_{yz}$	0.0002	$\beta_{yyz}$	0.0003
$\alpha_{zz}$	-72.5296	$\beta_{xyz}$	-0.0003
$\alpha_{\square}$	-7.87351	$\beta_{\text{tot}}$	5.5010
$\Delta\alpha$	9.086		

**Table 2 Optimized geometrical parameters of 2-chloro-5-nitrobenzaldehyde in two conformational states C<sub>1</sub> and C<sub>2</sub> obtained by HF/6-31G\*\* and DFT/6-31G\*\* calculation. The atoms numbered as shown in Fig1. The calculated energies between two conformers are reported.**

Parameters	Calculated values.				Experimental <sup>a</sup>
	C <sub>1</sub> conformer		C <sub>2</sub> conformer		
	HF	B3LYP	HF	DFT	
<i>Bond lengths (Å)</i>					
C <sub>1</sub> -C <sub>2</sub>	1.391	1.405	1.399	1.411	1.397
C <sub>1</sub> -C <sub>6</sub>	1.391	1.492	1.388	1.400	1.404
C <sub>1</sub> -C <sub>7</sub>	1.495	1.493	1.495	1.491	1.482
C <sub>2</sub> -C <sub>3</sub>	1.387	1.398	1.386	1.399	1.397
C <sub>2</sub> -Cl <sub>10</sub>	1.739	1.753	1.726	1.739	1.734
C <sub>3</sub> -C <sub>4</sub>	1.379	1.389	1.381	1.390	1.394
C <sub>3</sub> -H <sub>11</sub>	1.073	1.036	1.073	1.083	
C <sub>4</sub> -C <sub>5</sub>	1.385	1.396	1.381	1.393	1.397
C <sub>4</sub> -H <sub>12</sub>	1.072	1.083	1.072	1.083	1.094
C <sub>5</sub> -C <sub>6</sub>	1.375	1.385	1.378	1.387	1.383
C <sub>5</sub> -N <sub>13</sub>	1.458	1.474	1.456	1.471	
C <sub>6</sub> -H <sub>16</sub>	1.071	1.083	1.072	1.084	
C <sub>7</sub> -O <sub>8</sub>	1.888	1.214	1.184	1.210	
C <sub>7</sub> -H <sub>9</sub>	1.087	1.104	1.094	1.112	
N <sub>13</sub> -O <sub>14</sub>	1.191	1.228	1.192	1.229	
N <sub>13</sub> -O <sub>15</sub>	1.193	1.230	1.193	1.229	
<i>Bondangle (degree)</i>					
C <sub>2</sub> -C <sub>1</sub> -C <sub>6</sub>	118.521	118.433	118.254	118.183	
C <sub>2</sub> -C <sub>1</sub> -C <sub>7</sub>	123.852	123.850	126.011	125.944	
C <sub>6</sub> -C <sub>1</sub> -C <sub>7</sub>	117.626	117.716	115.735	115.873	
C <sub>1</sub> -C <sub>2</sub> -C <sub>3</sub>	121.408	121.344	120.658	120.677	
C <sub>1</sub> -C <sub>2</sub> -Cl <sub>10</sub>	121.237	121.083	122.437	122.106	
C <sub>3</sub> -C <sub>2</sub> -Cl <sub>10</sub>	117.355	117.572	116.905	117.217	
C <sub>2</sub> -C <sub>3</sub> -C <sub>4</sub>	119.678	119.696	120.506	120.452	
C <sub>2</sub> -C <sub>3</sub> -H <sub>11</sub>	119.828	119.717	119.354	119.213	
C <sub>4</sub> -C <sub>3</sub> -H <sub>11</sub>	119.677	120.586	120.139	120.334	
C <sub>3</sub> -C <sub>4</sub> -C <sub>5</sub>	119.827	118.933	118.744	118.787	
C <sub>3</sub> -C <sub>4</sub> -H <sub>12</sub>	120.494	121.499	121.022	121.529	
C <sub>5</sub> -C <sub>4</sub> -H <sub>12</sub>	118.905	119.567	120.232	119.684	
C <sub>4</sub> -C <sub>5</sub> -C <sub>6</sub>	121.010	121.884	121.419	121.474	
C <sub>4</sub> -C <sub>5</sub> -N <sub>13</sub>	120.083	118.861	119.394	119.298	
C <sub>6</sub> -C <sub>5</sub> -N <sub>13</sub>	121.884	119.254	119.186	119.226	
C <sub>1</sub> -C <sub>6</sub> -C <sub>5</sub>	118.925	119.709	120.418	120.425	
C <sub>5</sub> -C <sub>6</sub> -H <sub>16</sub>	119.190	119.063	120.275	120.285	
C <sub>1</sub> -C <sub>6</sub> -H <sub>16</sub>	121.084	121.227	119.306	119.288	
C <sub>1</sub> -C <sub>7</sub> -O <sub>8</sub>	122.121	122.542	126.582	126.655	
C <sub>1</sub> -C <sub>7</sub> -H <sub>9</sub>	116.744	116.103	112.769	112.346	
O <sub>8</sub> -C <sub>7</sub> -H <sub>9</sub>	121.133	121.354	120.648	120.998	
C <sub>5</sub> -N <sub>13</sub> -O <sub>14</sub>	117.597	117.543	117.438	117.415	
C <sub>5</sub> -N <sub>13</sub> -O <sub>15</sub>	117.324	117.306	117.528	117.508	
O <sub>14</sub> -N <sub>13</sub> -O <sub>15</sub>	125.078	125.149	125.033	125.076	
<i>Dihedral angle(degree)</i>					
C <sub>6</sub> -C <sub>1</sub> -C <sub>2</sub> -C <sub>3</sub>	0.000	0.0012	-0.0004	0.0013	
C <sub>6</sub> -C <sub>1</sub> -C <sub>2</sub> -Cl <sub>10</sub>	180.0005	180.003	-180.002	180.000	
C <sub>7</sub> -C <sub>1</sub> -C <sub>2</sub> -C <sub>3</sub>	180.004	180.002	180.000	180.012	
C <sub>7</sub> -C <sub>1</sub> -C <sub>2</sub> -Cl <sub>10</sub>	0.0009	0.0039	-0.0009	0.012	
C <sub>2</sub> -C <sub>1</sub> -C <sub>6</sub> -C <sub>5</sub>	-0.0003	-0.001	0.0005	-0.0004	
C <sub>2</sub> -C <sub>1</sub> -C <sub>6</sub> -H <sub>16</sub>	-180.0003	-180.000	180.000	-179.999	
C <sub>7</sub> -C <sub>1</sub> -C <sub>6</sub> -C <sub>5</sub>	179.999	-180.002	180.000	180.010	
C <sub>7</sub> -C <sub>1</sub> -C <sub>6</sub> -H <sub>16</sub>	-0.0007	-0.0016	-0.0004	-0.009	
C <sub>2</sub> -C <sub>1</sub> -C <sub>7</sub> -O <sub>8</sub>	180.0017	180.012	0.000	0.014	
C <sub>2</sub> -C <sub>1</sub> -C <sub>7</sub> -H <sub>9</sub>	0.002	0.014	179.999	180.012	
C <sub>6</sub> -C <sub>1</sub> -C <sub>7</sub> -O <sub>8</sub>	0.0022	0.0131	180.001	180.025	
C <sub>6</sub> -C <sub>1</sub> -C <sub>7</sub> -H <sub>9</sub>	180.002	180.015	0.0005	0.023	
C <sub>1</sub> -C <sub>2</sub> -C <sub>3</sub> -C <sub>4</sub>	0.0004	-0.0005	0.0	-0.001	
C <sub>1</sub> -C <sub>2</sub> -C <sub>3</sub> -H <sub>11</sub>	180.0006	179.999	179.999	-180.000	
Cl <sub>10</sub> -C <sub>2</sub> -C <sub>3</sub> -C <sub>4</sub>	179.999	-180.002	180.001	-180.000	
Cl <sub>10</sub> -C <sub>2</sub> -C <sub>3</sub> -H <sub>11</sub>	0.000	-0.0019	0.0005	-0.0002	
C <sub>2</sub> -C <sub>3</sub> -C <sub>4</sub> -C <sub>5</sub>	-0.000	-0.0004	0.0	-0.0001	
C <sub>2</sub> -C <sub>3</sub> -C <sub>4</sub> -H <sub>12</sub>	179.999	180.000	179.999	-180.000	
C <sub>11</sub> -C <sub>3</sub> -C <sub>4</sub> -C <sub>5</sub>	179.999	-180.000	180.001	-180.000	
C <sub>11</sub> -C <sub>3</sub> -C <sub>4</sub> -H <sub>12</sub>	-0.0005	-0.0003	0.001	0.000	
C <sub>3</sub> -C <sub>4</sub> -C <sub>5</sub> -C <sub>6</sub>	0.0	0.0005	0.0003	0.001	
C <sub>3</sub> -C <sub>4</sub> -C <sub>5</sub> -N <sub>13</sub>	-180.0	-179.999	179.999	180.000	

H12-C4-C5-C6	179.99	180.000	180.000	180.000
H12-C4-C5-N13	-0.0001	0.000	0.000	0.0002
C4-C5-C6-C1	0.0003	0.000	-0.0001	-0.000
C4-C5-C6-H16	180.000	179.999	179.999	-180.001
N13-C5-C6-C1	180.000	180.000	-179.999	180.0
N13-C5-C6-H16	0.0003	-0.0002	0.0	-0.0009
C4-C5-N13-O14	180.0	180.000	-0.0003	-0.002
C4-C5-N13-O15	0.0	0.0006	180.000	-180.002
C6-C5-N13-O14	0.0	0.0006	179.999	-180.00
C6-C5-N13-O15	180.000	180.000	-0.0002	-0.003
Energy (au)	-1005.8019	-1009.6466	-1005.7675	-1009.6583

<sup>a</sup>Geometric parameters determined with X-ray diffraction method from Refs.[44, 45, 46]

**Table 3 Definition of internal coordinates of 2-choloro-5-nitrobenzaldehyde**

No(i)	Symbol	Type	Definition
<i>Stretching</i>			
1-4	R <sub>i</sub>	C-H	C <sub>3</sub> -H <sub>11</sub> , C <sub>4</sub> -H <sub>12</sub> , C <sub>6</sub> -H <sub>16</sub> , C <sub>7</sub> -H <sub>9</sub>
5	r <sub>i</sub>	C-Cl	C <sub>2</sub> -Cl <sub>10</sub>
6	Q <sub>i</sub>	C-O	C <sub>7</sub> -O <sub>8</sub>
7	q <sub>i</sub>	C-N	C <sub>5</sub> -N <sub>13</sub>
8-4	S <sub>i</sub>	C-C	C <sub>1</sub> -C <sub>2</sub> , C <sub>2</sub> -C <sub>3</sub> , C <sub>3</sub> -C <sub>4</sub> , C <sub>4</sub> -C <sub>5</sub> , C <sub>5</sub> -C <sub>6</sub> , C <sub>6</sub> -C <sub>1</sub> , C <sub>1</sub> -C <sub>7</sub>
15-6	t <sub>i</sub>	N-O	N <sub>13</sub> -O <sub>14</sub> , N <sub>13</sub> -O <sub>15</sub>
<i>In-Plane Bending</i>			
17-22	α <sub>i</sub>	Ring	C <sub>1</sub> -C <sub>2</sub> -C <sub>3</sub> , C <sub>2</sub> -C <sub>3</sub> -C <sub>4</sub> , C <sub>3</sub> -C <sub>4</sub> -C <sub>5</sub> , C <sub>4</sub> -C <sub>5</sub> -C <sub>6</sub> , C <sub>5</sub> -C <sub>6</sub> -C <sub>1</sub> , C <sub>6</sub> -C <sub>1</sub> -C <sub>2</sub>
23-24	α <sub>i</sub>	C-C-C	C <sub>6</sub> -C <sub>1</sub> -C <sub>7</sub> , C <sub>2</sub> -C <sub>1</sub> -C <sub>7</sub>
25-30	β <sub>i</sub>	C-C-H	C <sub>4</sub> -C <sub>3</sub> -H <sub>11</sub> , C <sub>2</sub> -C <sub>3</sub> -H <sub>11</sub> , C <sub>5</sub> -C <sub>4</sub> -H <sub>12</sub> , C <sub>3</sub> -C <sub>4</sub> -H <sub>12</sub> , C <sub>5</sub> -C <sub>6</sub> -H <sub>16</sub> , C <sub>1</sub> -C <sub>6</sub> -H <sub>16</sub>
31	β <sub>i</sub>	C-C-H	C <sub>1</sub> -C <sub>7</sub> -H <sub>9</sub>
32	γ <sub>i</sub>	C-C-O	C <sub>1</sub> -C <sub>7</sub> -O <sub>8</sub>
33-34	γ <sub>i</sub>	C-C-Cl	C <sub>1</sub> -C <sub>2</sub> -Cl <sub>10</sub> , C <sub>3</sub> -C <sub>2</sub> -Cl <sub>10</sub>
35-36	θ <sub>i</sub>	C-C-N	C <sub>6</sub> -C <sub>5</sub> -N <sub>13</sub> , C <sub>4</sub> -C <sub>5</sub> -N <sub>13</sub>
37-38	φ <sub>i</sub>	C-N-O	C <sub>5</sub> -N <sub>13</sub> -O <sub>14</sub> , C <sub>5</sub> -N <sub>13</sub> -O <sub>15</sub>
39	Ψ <sub>i</sub>	O-N-O	O <sub>14</sub> -N <sub>13</sub> -O <sub>15</sub>
<i>Out-of-Plane Bending</i>			
40-43	ω <sub>i</sub>	C-H	H <sub>11</sub> -C <sub>3</sub> -C <sub>4</sub> -C <sub>2</sub> , H <sub>12</sub> -C <sub>4</sub> -C <sub>5</sub> -C <sub>3</sub> , H <sub>16</sub> -C <sub>6</sub> -C <sub>5</sub> -C <sub>1</sub> , H <sub>9</sub> -C <sub>7</sub> -C <sub>1</sub> -(C <sub>6</sub> , C <sub>2</sub> )
44	ε <sub>i</sub>	C-Cl	Cl <sub>10</sub> -C <sub>2</sub> -C <sub>1</sub> -C <sub>3</sub>
45	μ <sub>i</sub>	C-N	N <sub>13</sub> -C <sub>5</sub> -C <sub>6</sub> -C <sub>4</sub>
46	λ <sub>i</sub>	C-O	O <sub>8</sub> -C <sub>7</sub> -C <sub>1</sub> -(C <sub>6</sub> , C <sub>2</sub> )
<i>Torsion</i>			
47-53	τ <sub>i</sub>	t Ring	C <sub>1</sub> -C <sub>2</sub> -C <sub>3</sub> -C <sub>4</sub> , C <sub>2</sub> -C <sub>3</sub> -C <sub>4</sub> -C <sub>5</sub> , C <sub>3</sub> -C <sub>4</sub> -C <sub>5</sub> -C <sub>6</sub> , C <sub>4</sub> -C <sub>5</sub> -C <sub>6</sub> -C <sub>1</sub> , C <sub>5</sub> -C <sub>6</sub> -C <sub>1</sub> -C <sub>2</sub> , C <sub>6</sub> -C <sub>1</sub> -C <sub>2</sub> -C <sub>3</sub> , C <sub>7</sub> -C <sub>1</sub> -C <sub>6</sub> -C <sub>2</sub>
54	τ <sub>i</sub>	N-O	C <sub>5</sub> -N <sub>13</sub> -(O <sub>14</sub> , O <sub>15</sub> )-(C <sub>6</sub> , C <sub>4</sub> )

**Table 4 Definition of local symmetry coordinates of 2-choloro-5-nitrobenzaldehyde**

No(i)	Symbol <sup>a</sup>	Definition <sup>b</sup>
1-4	CH	R <sub>1</sub> , R <sub>2</sub> , R <sub>3</sub> , R <sub>4</sub>
5	CCl	r <sub>5</sub>
6	CO	Q <sub>6</sub>
7	CN	q <sub>7</sub>
8-14	CC	S <sub>8</sub> , S <sub>9</sub> , S <sub>10</sub> , S <sub>11</sub> , S <sub>12</sub> , S <sub>13</sub> , S <sub>14</sub>
15	NO <sub>2</sub> symd	(t <sub>15</sub> +t <sub>16</sub> )/√2
16	NO <sub>2</sub> asymd	(t <sub>15</sub> - t <sub>16</sub> )/√2
17	R trigd	(α <sub>17</sub> - α <sub>18</sub> +α <sub>19</sub> - α <sub>20</sub> +α <sub>21</sub> - α <sub>22</sub> )/√6
18	R symd	(-α <sub>17</sub> - α <sub>18</sub> +2α <sub>19</sub> - α <sub>20</sub> - α <sub>21</sub> +2α <sub>22</sub> )/√12
19	R asymd	(α <sub>17</sub> - α <sub>18</sub> + α <sub>20</sub> - α <sub>21</sub> )/2
20	b CC	(α <sub>23</sub> - α <sub>24</sub> )/√2
21-23	b CH	(β <sub>25</sub> - β <sub>26</sub> )/√2, (β <sub>27</sub> - β <sub>28</sub> )/√2, (β <sub>29</sub> - β <sub>30</sub> )/√2
24	b CH	β <sub>31</sub>
25	b CO	γ <sub>32</sub>
26	b CCl	(γ <sub>33</sub> - γ <sub>34</sub> )/√2
27	b CN	(θ <sub>35</sub> - θ <sub>36</sub> )/√2
28	NO <sub>2</sub> rock	(φ <sub>37</sub> - φ <sub>38</sub> )/√2
29	NO <sub>2</sub> twist	(φ <sub>37</sub> +φ <sub>38</sub> )/√2
30	NO <sub>2</sub> scis	(2Ψ <sub>39</sub> - φ <sub>37</sub> - φ <sub>38</sub> )/√6
31-34	ω CH	ω <sub>40</sub> , ω <sub>41</sub> , ω <sub>42</sub> , ω <sub>43</sub>
35	ε CCl	ε <sub>44</sub>
36	μ CN	μ <sub>45</sub>
37	λ CO	λ <sub>46</sub>
38	tR trigd	(τ <sub>47</sub> - τ <sub>48</sub> +τ <sub>49</sub> - τ <sub>50</sub> +τ <sub>51</sub> - τ <sub>52</sub> )/√6
49	tR symd	(τ <sub>47</sub> - τ <sub>49</sub> +τ <sub>40</sub> - τ <sub>52</sub> )/√2
40	tR asymd	(-τ <sub>47</sub> +2τ <sub>48</sub> - τ <sub>49</sub> - τ <sub>40</sub> +2τ <sub>51</sub> - τ <sub>52</sub> )/√12
41	t CC	τ <sub>53</sub>
42	t NO <sub>2</sub> wag	τ <sub>54</sub>

<sup>a</sup>These symbols are used for description of the normal modes by PED in Table 4<sup>b</sup>The internal coordinates used here are defined in Table 2

Table 5 Observed and, Calculated wave numbers and intensities (km mol<sup>-1</sup> for IR and Å<sup>4</sup> am<sup>-1</sup> for Raman) of 2-choloro-5-nitrobenzaldehyde

Mode	species	Observed frequency (cm <sup>-1</sup> )		Calculated Frequency (cm <sup>-1</sup> )					IR Intensity				Raman activity				Assignments <sup>a</sup> (%PED)	
				Unscaled				Scaled	C <sub>1</sub>		C <sub>2</sub>		C <sub>1</sub>		C <sub>2</sub>			
		FT-IR	Raman	C <sub>1</sub>		C <sub>2</sub>			HF	B3LYP	HF	B3LYP	HF	B3LYP	HF	B3LYP		HF
				HF	B3LYP	HF	B3LYP											
1.	A'	3100(vs)	3096(w)	3428	3248	3422	3248	3118	16.06	4.26	3.44	3.95	33.23	95.27	85.19	95.69	vCH(99)	
2.	A'	2980(s)		3423	3243	3405	3227	2984	8.54	13.86	3.06	0.91	86.62	44.50	51.93	92.48	vCH(99)	
3.	A'	2920(s)	2917(vw)	3396	3228	3396	3223	2918	0.46	0.39	0.45	2.52	64.73	70.08	56.82	27.06	vCH(99)	
4.	A'	2860(ms)		3238	3003	3147	2908	2852	46.67	57.82	81.94	96.05	79.51	93.01	86.62	97.82	vCH(99)	
5.	A'	1771(w)	1778(w)	2002	1796	2027	1718	1775	294.03	183.89	289.99	200.98	53.19	60.08	58.97	65.93	vCO(87)+CC(5)	
6.	A'	1695(vs)	1695(vs)	1873	1674	1871	1671	1708	441.30	169.02	498.15	192.80	2.47	11.47	2.40	12.17	NO <sub>2</sub> asym(56)+NO <sub>2</sub> sci(24)+CN(14)	
7.	A'	1610(s)	1608(w)	1792	1631	1794	1634	1617	61.76	47.15	58.78	64.02	88.22	103.46	83.56	98.71	vCC(43)+bCN(17)+NO <sub>2</sub> asy(12)	
8.	A'	1590(w)	1586(s)	1762	1613	1756	1607	1612	33.68	44.65	8.26	14.89	17.73	27.74	32.59	42.35	vCC(52)+bCH(23)+bRing(15)	
9.	A'	1465(vw)		1652	1495	1655	1501	1469	126.18	38.19	89.25	37.43	85.18	0.320	60.79	1.42	bCH(59)+CC(25)	
10.	A'	1400(w)	1397(w)	1629	1442	1632	1458	1404	231.24	8.24	318.40	3.41	30.71	7.37	80.60	1.82	bCH(54)+CC(13)+ bRing (5)	
11.	A'	1357(vs)	1357(vw)	1562	1432	1579	1421	1361	9.59	25.18	7.37	5.04	2.25	16.33	1.53	8.04	vCC(34)+NO <sub>2</sub> asy(24)+bCH(15)	
12.	A'	1351(s)	1354(vs)	1551	1398	1540	1398	1350	83.36	337.49	23.79	356.85	4.97	213.58	0.97	172.13	NO <sub>2</sub> asym(37)+CC(33)+bCH(14)	
13.	A'	1303(w)	1304(w)	1386	1357	1391	1365	1309	48.39	5.75	17.01	42.34	2.27	5.48	0.69	12.49	vCC(47)+bCH(35)+ bRing (5)	
14.	A'	1252(vw)		1331	1268	1347	1274	1254	47.53	40.72	103.68	15.09	23.16	1.94	35.61	0.75	bCH(71)+gRing(15)+gCN(7)	

15.	A'	1190(s)	1193(vw)	1277	1208	1279	1212	1195	5.21	40.52	9.93	49.10	18.68	54.61	20.95	58.53	vCC(59)+bCH(22)+CCI(16)
16.	A'	1144(w)	1147(w)	1245	1159	1246	1159	1150	0.10	5.13	8.61	1.25	4.89	14.40	0.89	8.37	bCH(80)
17.	A'	1098(w)	1100(vw)	1221	1109	1227	1128	1099	8.53	17.77	1.22	22.54	8.53	17.77	6.14	5.78	vCC(45)+CN(16)+bCH(14)+NO <sub>2</sub> sym(11)
18.	A'	1072(vw)	1072(w)	1152	1062	1174	1078	1075	93.12	99.56	95.11	105.51	93.12	99.56	16.33	26.21	vCC(40)+ bRing (14)+CN(8)+bCO(6)
19.	A''	1002(vs)	1004(w)	1149	1034	1144	1026	1004	0.45	0.97	0.08	0.36	0.45	0.97	7.56	6.92	gCH(71)+ gRing (15)+gCN(7)
20.	A''	942(w)	945(w)	1120	992	1121	995	946	0.00	0.17	0.00	0.19	0.00	0.17	1.30	1.08	gCH(80)+ gRing (6)
21.	A''	920(s)		1082	966	1059	942	924	11.43	9.50	13.56	11.51	11.43	9.50	1.46	0.95	gCH(80)+NO <sub>2</sub> Wag(15)
22.	A'			1041	954	1026	937	587	48.43	51.48	41.78	51.73	48.43	51.48	6.62	4.75	NO <sub>2</sub> sci.(32)+CC(29)+bCH(6)
23.	A''	846(w)		957	857	962	862	850	17.22	15.35	17.32	14.68	17.22	15.35	1.12	2.29	gCH(80)+NO <sub>2</sub> Wag(15)
24.	A'	835(w)	839(w)	914	828	913	831	838	29.42	29.01	30.60	25.13	29.42	29.01	3.87	9.33	vCN(40)+CCI(17)+ bRing (16)+CC(13)
25.	A'	740(s)	743(s)	855	751	855	751	744	47.94	23.59	48.80	23.72	47.94	23.59	3.21	1.64	NO <sub>2</sub> wag(47)+gCH(37)+gCN(9)
26.	A'			800	740	789	729	721	16.31	11.25	53.34	38.56	16.31	11.25	2.68	1.72	bCC(24)+NO <sub>2</sub> roc(18)+ bRing (17)+bCO(12)
27.	A''			782	705	784	707	675	0.02	0.99	0.03	1.45	0.02	0.99	0.12	0.88	gRing (37)+gCC(25)+gCCI(13)+gCH(10)
28.	A'	645(vw)	648(vw)	700	650	745	691	647	12.64	9.42	11.19	8.39	12.64	9.42	8.48	7.01	bRring (38)+CC(25)+bCO(19)CCI(9)
29.	A'	534(vw)	539(w)	587	541	627	577	536	11.00	7.31	19.70	16.15	11.00	7.31	2.70	2.66	bCN(31)+NO <sub>2</sub> roc(28)+bCCI(18)+bCC(8 )
30.	A'	521(w)	520(w)	568	521	586	539	525	55.61	37.65	10.69	7.67	55.61	37.65	1.68	2.57	vCCI(39)+CN(26)+bCO(12)+CC(12)
31.	A''			567	519	876	530	527	0.60	0.18	0.42	0.10	0.60	0.18	0.27	0.49	gCN(35)+ gRing (18)+gCN(17)+gCH(17)
32.	A'	495(w)	495(w)	533	494	491	450	498	3.15	3.83	2.39	1.14	3.15	3.83	0.01	0.00	bRing (55)+CC(21)+bCH(13)

33.	A''		498	459	414	384	366	6.83	2.97	0.99	0.52	6.83	2.97	5.10	6.68	gCC(63)+gCCI(14)+gCN(8)
34.	A'	330(s)	353	325	382	354	332	3.18	2.63	5.45	3.62	3.17	2.63	1.09	0.91	bCO(23)NO <sub>2</sub> roc(21)+bCCI(19)+bCN(17)
35.	A'	316(w)	335	308	341	314	319	1.59	0.84	0.01	0.32	1.58	0.84	4.27	3.11	bRing(34)+CC(18)+bCO(15)
36.	A''	295(w)	331	302	327	296	293	7.02	4.58	5.46	3.45	0.91	0.30	1.97	1.26	gRing(34)+gCN(33)+gCCI(11)+gCC(7)
37.	A'	220(w)	233	214	230	220	222	4.19	3.07	0.13	2.56	1.63	1.71	0.70	0.16	bCCI(36)+bCN(20)+bCC(17)+CC(16)+ NO <sub>2</sub> roc(7)
38.	A''	200(vw)	198	182	228	212	204	1.47	1.27	3.47	0.19	2.84	2.62	0.39	0.71	gRing(65)+gCH(14)+gCCI(12)+gCN(5)
39.	A'	183(vw)	177	161	193	176	185	1.97	1.53	11.68	7.85	0.10	0.19	0.68	0.32	NO <sub>2</sub> roc.(39)+ gRing (29)+gCH(18)+bCO(14)
40.	A''		114	123	101	94	114	18.58	9.34	11.69	11.01	0.57	1.18	0.82	1.41	gCO(38) +bCCI(30) +gCH(17) + gRing (8) +gCN(7)
41.	A''		97	88	75	84	95	0.90	2.54	5.55	0.02	1.07	1.07	1.67	1.57	gCCI(36)+gCN(19)+ gRing (13)+gCH(9)
42.	A''		48	53	51	54	50	0.37	0.17	1.43	0.54	0.84	0.08	1.42	0.95	NO <sub>2</sub> tor.(36) +bCN(25) +gCC(20) +gCC(19)

<sup>a</sup>Assignments: v-Stretching ; b-in- plane bending ; g-out-of-plane bending; sci.- scissoring; roc.- rocking; wag. – wagging; tor.-torsion.

**Table 6 NBO results showing the formation of Lewis and non Lewis orbital's-----the valence hybrids corresponding to the intramolecular NO<sub>2</sub> .....Cl Hydrogen bonds in CNB.**

BOND(A-B)	ED/ ENERGY (a.u)	ED <sub>A</sub> (%)	ED <sub>B</sub> (%)	NBO	S(%)	P(%)
BD(1)C1-C2	1.97947	49.92	50.08	0.7065(sp <sup>1.87</sup> ) <sub>C+</sub>	34.87	65.09
				0.7077(sp <sup>1.60</sup> ) <sub>C</sub>	38.44	61.52
BD(1)C1-C6	1.96576	50.90	49.10	0.7134(sp <sup>1.79</sup> ) <sub>C+</sub>	35.80	64.17
				0.7007(sp <sup>1.86</sup> ) <sub>C</sub>	34.97	64.99
BD(1)C1-C7	1.98065	54.24	45.76	0.7365(sp <sup>2.41</sup> ) <sub>C+</sub>	29.32	70.65
				0.6765(sp <sup>1.90</sup> ) <sub>C</sub>	34.47	65.47
BD(1)C2-C3	1.98144	51.10	48.90	0.7148(sp <sup>1.58</sup> ) <sub>C+</sub>	38.77	61.19
				0.6993(sp <sup>1.91</sup> ) <sub>C</sub>	34.31	65.65
BD(1)C2-Cl10	1.98895	46.02	53.98	0.6784(sp <sup>3.39</sup> ) <sub>C+</sub>	22.72	77.13
				0.7347(sp <sup>4.72</sup> ) <sub>Cl</sub>	17.40	82.14
BD(1)C3-C4	1.96944	50.04	49.96	0.7074(sp <sup>1.85</sup> ) <sub>C+</sub>	35.07	64.89
				0.7068(sp <sup>1.84</sup> ) <sub>C</sub>	35.19	64.77
BD(1)C3-H11	1.96944	63.40	36.60	0.7963(sp <sup>2.27</sup> ) <sub>C+</sub>	30.59	69.38
BD(1)C4-C5	1.97788	49.12	50.88	0.6050(sp <sup>0.00</sup> ) <sub>H</sub>	99.95	0.05
				0.7009(sp <sup>1.94</sup> ) <sub>C+</sub>	34.05	65.90
BD(1)C4-H12	1.97764	64.03	35.97	0.7133(sp <sup>1.68</sup> ) <sub>C</sub>	37.25	62.72
				0.8002(sp <sup>2.25</sup> ) <sub>C+</sub>	30.72	69.25
BD(1)C5-C6	1.97630	50.82	49.18	0.5998(sp <sup>0.00</sup> ) <sub>H</sub>	99.94	0.06
				0.7129(sp <sup>1.68</sup> ) <sub>C+</sub>	37.33	62.64
BD(1)C5-N13	1.98940	38.25	61.75	0.7013(sp <sup>1.94</sup> ) <sub>C</sub>	34.02	65.93
				0.6185(sp <sup>2.94</sup> ) <sub>C+</sub>	25.34	74.52
BD(1)C6-H16	1.97505	64.82	35.18	0.7858(sp <sup>1.83</sup> ) <sub>N</sub>	35.37	64.59
				0.8051(sp <sup>2.23</sup> ) <sub>C+</sub>	30.98	68.99
BD(1)C7-O8	1.99727	34.15	65.85	0.5931(sp <sup>0.00</sup> ) <sub>H</sub>	99.94	0.06
				0.8115(sp <sup>2.17</sup> ) <sub>C+</sub>	31.48	68.40
BD(1)C7-H9	1.98845	60.57	39.43	0.8115(sp <sup>1.47</sup> ) <sub>O</sub>	40.39	59.24
				0.7783(sp <sup>1.93</sup> ) <sub>C+</sub>	34.12	65.82
BD(1)N13-O14	1.99585	48.19	51.81	0.6279(sp <sup>0.00</sup> ) <sub>H</sub>	99.94	0.06
				0.6942(sp <sup>2.10</sup> ) <sub>N+</sub>	32.29	67.66
BD(1)N13-O15	1.99584	48.15	51.85	0.7198(sp <sup>2.67</sup> ) <sub>O</sub>	27.14	72.46
				0.6939(sp <sup>2.10</sup> ) <sub>N+</sub>	32.27	67.69
BD* (1)C1-C2	0.03287	50.08	49.92	0.7201(sp <sup>2.66</sup> ) <sub>O</sub>	27.20	72.40
				0.7077(sp <sup>1.87</sup> ) <sub>C+</sub>	34.87	65.09
BD* (1)C1-C6	0.02144	49.10	50.90	-0.7065(sp <sup>1.60</sup> ) <sub>C</sub>	34.44	61.52
				0.7007(sp <sup>1.79</sup> ) <sub>C+</sub>	35.80	64.17
BD* (1)C1-C7	0.07116	45.76	54.24	-0.7134(sp <sup>1.86</sup> ) <sub>C</sub>	34.97	64.99
				0.6765(sp <sup>2.41</sup> ) <sub>C+</sub>	29.32	70.65
BD* (1)C2-Cl10	0.03233	53.98	46.02	-0.7365(sp <sup>1.90</sup> ) <sub>C</sub>	34.47	65.47
				0.7347(sp <sup>3.39</sup> ) <sub>C+</sub>	22.72	77.13
BD* (1)C3-C4	0.01547	49.96	50.04	-0.6784(sp <sup>4.42</sup> ) <sub>Cl</sub>	17.40	82.14
				0.7068(sp <sup>1.85</sup> ) <sub>C+</sub>	35.07	64.89
BD* (1)C3-H11	0.01177	36.60	63.404	-0.7074(sp <sup>1.84</sup> ) <sub>C</sub>	35.19	64.77
				0.6050(sp <sup>2.27</sup> ) <sub>C+</sub>	30.59	69.38
BD* (1)C4-C5	0.02219	50.88	49.12	-0.7963(sp <sup>0.00</sup> ) <sub>H</sub>	99.95	0.05
				0.7133(sp <sup>1.94</sup> ) <sub>C+</sub>	34.05	65.90
BD* (1)C4-H12	0.01272	35.97	64.03	-0.7009(sp <sup>1.68</sup> ) <sub>C</sub>	37.25	62.72
				0.5998(sp <sup>2.25</sup> ) <sub>N+</sub>	30.23	69.73
BD* (1)C5-C6	0.02070	49.18	50.82	-0.8002(sp <sup>0.00</sup> ) <sub>H</sub>	99.94	0.06
				0.7013(sp <sup>1.94</sup> ) <sub>C</sub>	34.02	65.93
BD* (1)C5-N13	0.11581	61.75	38.25	0.7858(sp <sup>2.90</sup> ) <sub>C+</sub>	25.34	74.52
				-0.6185(sp <sup>1.83</sup> ) <sub>N</sub>	35.37	64.59
BD* (1)C2-C3	0.02632	48.90	51.10	0.6993(sp <sup>1.58</sup> ) <sub>C+</sub>	38.77	61.19
				-0.7148(sp <sup>1.91</sup> ) <sub>C</sub>	34.31	65.65
BD* (1)C6-H16	0.01638	35.18	64.82	0.5931(sp <sup>2.23</sup> ) <sub>C+</sub>	30.98	68.99
				-0.8051(sp <sup>0.00</sup> ) <sub>H</sub>	99.94	0.06
BD* (1)C7-O8	0.00311	65.85	34.15	0.8115(sp <sup>2.21</sup> ) <sub>C+</sub>	31.48	68.40
				-0.5844(sp <sup>1.47</sup> ) <sub>O</sub>	40.39	59.24
BD* (1)C7-H9	0.05529	39.43	60.57	0.6279(sp <sup>1.97</sup> ) <sub>C+</sub>	34.12	65.82
				-0.7783(sp <sup>0.00</sup> ) <sub>H</sub>	99.94	0.06
BD* (1)N13-O14	0.05612	51.81	48.19	0.7198(sp <sup>2.10</sup> ) <sub>N+</sub>	32.29	67.66
				-0.6942(sp <sup>2.67</sup> ) <sub>O</sub>	27.14	72.46
BD* (1)N13-O15	0.05634	51.85	48.15	0.7201(sp <sup>2.10</sup> ) <sub>N+</sub>	32.27	67.69
				-0.6939(sp <sup>2.66</sup> ) <sub>O</sub>	27.20	72.40
LP (1) O8	1.98400	---	---	sp <sup>0.68</sup>	59.60	40.36
LP (1) C1	1.99303	---	---	sp <sup>0.21</sup>	82.58	17.41
LP (1) O14	1.98011	---	---	sp <sup>0.37</sup>	72.89	27.09
LP (1) O15	1.98011	---	---	sp <sup>0.37</sup>	72.83	27.15

**Table 7 The second order perturbation energies  $E^{(2)}$  (kcal/mol) corresponding to the most important charge transfer interactions (donor-acceptor) in the compounds studied by B3LYP/ 6-31G\*\*method**

Donor NBO (i)	Acceptor NBO (j)	$E^{(2)}$ (kcal/mol)	$\frac{E(j)-E(i)}{(\text{a.u})}$	$F(i,j)$ (a.u)
BD(1)C1-C2	BD*(1)C1-C6	3.58	1.31	0.061
BD(1)C1-C2	BD*(1)C1-C7	1.32	1.12	0.035
BD(1)C1-C2	BD*(1)C2-C3	3.62	1.29	0.061
BD(1)C1-C2	BD*(1)C3-H11	2.00	1.24	0.044
BD(1)C1-C2	BD*(1)C6-H16	1.66	1.25	0.041
BD(1)C1-C2	BD*(1)C7-O8	0.75	1.32	0.028
BD(1)C1-C6	BD*(1)C1-C2	4.42	1.27	0.067
BD(1)C1-C6	BD*(1)C1-C7	1.20	1.09	0.033
BD(1)C1-C6	BD*(1)C2-C110	4.55	0.84	0.055
BD(1)C1-C6	BD*(1)C5-C6	2.59	1.27	0.051
BD(1)C1-C6	BD*(1)C5-N13	4.26	1.00	0.059
BD(1)C1-C6	BD*(1)C6-H16	1.53	1.23	0.039
BD(1)C1-C6	BD*(1)C7-H9	0.64	1.14	0.024
BD(1)C1-C7	BD*(1)C1-C2	1.55	1.19	0.038
BD(1)C1-C7	BD*(1)C5-C6	2.64	1.19	0.050
BD(1)C2-C3	BD*(1)C3-H11	1.60	1.23	0.040
BD(1)C2-C3	BD*(1)C4-H12	1.78	1.24	0.042
BD(1)C2-C110	BD*(1)C3-C4	2.22	1.28	0.048
BD(1)C3-C4	BD*(1)C2-C110	4.79	0.84	0.057
BD(1)C3-C4	BD*(1)C4-C5	2.59	1.26	0.051
BD(1)C3-C4	BD*(1)C5-N13	4.41	1.00	0.060
BD(1)C3-H11	BD*(1)C4-C5	3.71	1.09	0.057
BD(1)C6-H16	BD*(1)C1-C2	4.74	1.08	0.061
BD(1)C6-H16	BD*(1)C5-N13	0.62	0.82	0.021
BD(1)C7-O8	BD*(1)C1-C2	1.04	1.60	0.037
BD(1)N13-O14	BD*(1)C5-N13	0.85	1.40	0.032
BD(1)N13-O15	BD*(1)C5-N13	0.85	1.40	0.032
BD(1)N13-O15	BD*(1)C5-C6	0.76	1.68	0.032
BD(1)C6-H16	BD*(1)C4-C5	4.32	1.08	0.061
BD(1)C4-C5	BD*(1)N13-O14	2.11	1.21	0.045
BD(1)C4-H12	BD*(1)C5-N13	0.61	0.82	0.020
LP(1) C110	BD*(1)C2-C3	1.13	1.47	0.036
LP(1) C110	BD*(1)C1-C2	1.51	1.48	0.042
LP(1) O14	BD*(1)C5-N13	4.46	1.05	0.063
LP(1) O14	BD*(1)N13-O15	2.55	1.25	0.05
LP(1) O15	BD*(1)C5-N13	4.45	1.05	0.063
LP(1) O15	BD*(1)N13-O14	2.54	1.25	0.051

**Table 8 Selected HOMO, LUMO energies of 2-chloro-5-nitrobenzaldehyde.**

S No	Molecular orbitals	Energy a.u.
1	HOMO	-0.27894
2	HOMO-1	-0.29305
3	HOMO-2	-0.30175
4	LUMO	-0.10299
5	LUMO+1	-0.08980
6	LUMO+2	-0.02878

**Table 9 Selected HOMO-LUMO energy gap of 2-chloro5-nitrobenzaldehyde.**

S No	Molecular orbital Energy transitions	Energy gap a.u.
1	HOMO→LUMO	-0.17595
2	HOMO-1→LUMO	-0.18914
3	HOMO-2→LUMO	-0.25016
4	HOMO→LUMO	-0.18006
5	HOMO-1→LUMO+1	-0.20325
6	HOMO-2→LUMO+1	-0.26427
7	HOMO→LUMO	-0.19876
8	HOMO-1→LUMO+2	-0.21175
9	HOMO-2→LUMO+2	-0.27297